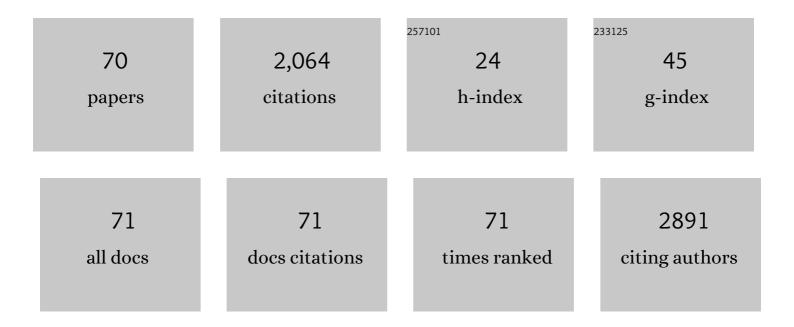
List of Publications by Year in descending order

Source: https://exaly.com/author-pdf/3191449/publications.pdf Version: 2024-02-01



KALCHEN

#	Article	IF	CITATIONS
1	Rayleigh anomaly-enabled mode hybridization in gold nanohole arrays by scalable colloidal lithography for highly-sensitive biosensing. Nanophotonics, 2022, 11, 507-517.	2.9	14
2	Cylindrical vector beams reveal radiationless anapole condition in a resonant state. Opto-Electronic Advances, 2022, 5, 210014-210014.	6.4	21
3	Morphology Effect of Bismuth Vanadate on Electrochemical Sensing for the Detection of Paracetamol. Nanomaterials, 2022, 12, 1173.	1.9	8
4	Etching-free high-throughput intersectional nanofabrication of diverse optical nanoantennas for nanoscale light manipulation. Journal of Colloid and Interface Science, 2022, 622, 950-959.	5.0	6
5	Cylindrical vector beam revealing multipolar nonlinear scattering for superlocalization of silicon nanostructures. Photonics Research, 2021, 9, 950.	3.4	7
6	Ultra-narrow-band metamaterial perfect absorber based on surface lattice resonance in a WS <sub>2</sub> nanodisk array. Optics Express, 2021, 29, 27084.	1.7	27
7	Nanoantenna Structure with Mid-Infrared Plasmonic Niobium-Doped Titanium Oxide. Micromachines, 2020, 11, 23.	1.4	5
8	Anapole mediated giant photothermal nonlinearity in nanostructured silicon. Nature Communications, 2020, 11, 3027.	5.8	69
9	Enhanced photocurrent generation from indium–tin-oxide/Fe2TiO5 hybrid nanocone arrays. Nano Energy, 2020, 76, 104965.	8.2	9
10	Loss-favored ultrasensitive refractive index sensor based on directional scattering from a single all-dielectric nanosphere. Journal of Materials Chemistry C, 2020, 8, 6350-6357.	2.7	3
11	Flexible microbubble-based Fabry–Pérot cavity for sensitive ultrasound detection and wide-view photoacoustic imaging. Photonics Research, 2020, 8, 1558.	3.4	19
12	Photocurrent Enhancements of TiO <sub>2</sub> -Based Nanocomposites with Gold Nanostructures/Reduced Graphene Oxide on Nanobranched Substrate. Journal of Physical Chemistry C, 2019, 123, 21103-21113.	1.5	33
13	High quality thermochromic VO2 films prepared by magnetron sputtering using V2O5 target with in situ annealing. Applied Surface Science, 2019, 495, 143436.	3.1	44
14	Ultra-Narrow Band Mid-Infrared Perfect Absorber Based on Hybrid Dielectric Metasurface. Nanomaterials, 2019, 9, 1350.	1.9	30
15	Structure and optical properties of sputter deposited pseudobrookite Fe <sub>2</sub> TiO <sub>5</sub> thin films. CrystEngComm, 2019, 21, 34-40.	1.3	30
16	High-sensitivity and fast-response fiber-tip Fabry–Pérot hydrogen sensor with suspended palladium-decorated graphene. Nanoscale, 2019, 11, 15821-15827.	2.8	49
17	Indium–Tin–Oxide Nanostructures for Plasmon-Enhanced Infrared Spectroscopy: A Numerical Study. Micromachines, 2019, 10, 241.	1.4	6
18	Dual-band <i>in situ</i> molecular spectroscopy using single-sized Al-disk perfect absorbers. Nanoscale, 2019, 11, 9508-9517.	2.8	22

#	Article	IF	CITATIONS
19	Selective thermal emitters with infrared plasmonic indium tin oxide working in the atmosphere. Optical Materials Express, 2019, 9, 2534.	1.6	20
20	Ultra-Broadband Directional Scattering by Colloidally Lithographed High-Index Mie Resonant Oligomers and Their Energy-Harvesting Applications. ACS Applied Materials & Interfaces, 2018, 10, 16776-16782.	4.0	34
21	Metal/Conductive Oxide Plasmonic Structures for Surface-Enhanced Infrared Absorption Spectroscopy. Bunseki Kagaku, 2018, 67, 81-94.	0.1	1
22	High- <i>Q</i> , low-mode-volume and multiresonant plasmonic nanoslit cavities fabricated by helium ion milling. Nanoscale, 2018, 10, 17148-17155.	2.8	22
23	Ultra-narrow Nanoslit Cavities for High-Q Resonances in the Visible Range. , 2018, , .		0
24	Enhanced photoelectrochemical water splitting by plasmonic Au nanostructures/reduced graphene oxide. , 2018, , .		0
25	Al nanoantennas for plasmon-enhanced infrared spectroscopy. , 2018, , .		0
26	Resonant Optical Absorption and Photothermal Process in High Refractive Index Germanium Nanoparticles. Advanced Optical Materials, 2017, 5, 1600902.	3.6	34
27	UV-visible light photocurrent enhancement in STO thin films through metal-defect co-doping effect combined with Au plasmons. Materials Express, 2017, 7, 66-71.	0.2	1
28	Proteinâ€Functionalized Indiumâ€Tin Oxide Nanoantenna Arrays for Selective Infrared Biosensing. Advanced Optical Materials, 2017, 5, 1700091.	3.6	23
29	Tunable Nanoantennas for Surface Enhanced Infrared Absorption Spectroscopy by Colloidal Lithography and Post-Fabrication Etching. Scientific Reports, 2017, 7, 44069.	1.6	37
30	Far-field and near-field monitoring of hybridized optical modes from Au nanoprisms suspended on a graphene/Si nanopillar array. Nanoscale, 2017, 9, 16950-16959.	2.8	10
31	Nanowire-plasmonic photocatalysts and thermal emitters. , 2017, , .		0
32	Effects of nanoscale morphology and defects in oxide: optoelectronic functions of zinc oxide nanowires. Radiation Effects and Defects in Solids, 2016, 171, 22-33.	0.4	9
33	Aluminum infrared plasmonic perfect absorbers for wavelength selective devices. Proceedings of SPIE, 2016, , .	0.8	1
34	Spectrally Selective Midâ€Infrared Thermal Emission from Molybdenum Plasmonic Metamaterial Operated up to 1000 °C. Advanced Optical Materials, 2016, 4, 1987-1992.	3.6	79
35	Ensemble of gold-patchy nanoparticles with multiple hot-spots for plasmon-enhanced vibrational spectroscopy. Proceedings of SPIE, 2016, , .	0.8	2
36	Hole Array Perfect Absorbers for Spectrally Selective Midwavelength Infrared Pyroelectric Detectors. ACS Photonics, 2016, 3, 1271-1278.	3.2	92

#	Article	IF	CITATIONS
37	Electromechanically Tunable Suspended Optical Nanoantenna. Nano Letters, 2016, 16, 2680-2685.	4.5	18
38	Solar water heating and vaporization with silicon nanoparticles at mie resonances. Optical Materials Express, 2016, 6, 640.	1.6	69
39	High Temperature Wavelength-Selective Thermal Emitters Based on Metal-Insulator-Metal Structures. Hyomen Kagaku, 2016, 37, 380-385.	0.0	1
40	Fabrication and Characterization of MoirÃ $ m{O}$ Metasurfaces. , 2016, , .		0
41	Plasmon mediated cathodic photocurrent generation in sol-gel synthesized doped SrTiO3 nanofilms. APL Materials, 2015, 3, .	2.2	6
42	Infrared Aluminum Metamaterial Perfect Absorbers for Plasmonâ€Enhanced Infrared Spectroscopy. Advanced Functional Materials, 2015, 25, 6637-6643.	7.8	129
43	Excitation Induced Tunable Emission in Ce <sup><b>3+</b></sup> /Eu <sup><b>3+</b></sup> Codoped BiPO <sub><b>4</b></sub> Nanophosphors. Journal of Spectroscopy, 2015, 2015, 1-10.	0.6	14
44	Infrared Perfect Absorbers Fabricated by Colloidal Mask Etching of Al–Al <sub>2</sub> O <sub>3</sub> –Al Trilayers. ACS Photonics, 2015, 2, 964-970.	3.2	172
45	Moiré Nanosphere Lithography. ACS Nano, 2015, 9, 6031-6040.	7.3	91
46	Lossy plasmonic resonances in nanoparticles for broadband light absorption. , 2015, , .		0
47	Aluminum infrared plasmonic perfect absorbers fabricated by colloidal lithography. , 2015, , .		1
48	Moir $ ilde{A}$ © nanosphere lithography: use colloidal moir $ ilde{A}$ © patterns as masks. Proceedings of SPIE, 2015, , .	0.8	1
49	Transparent oxides forming conductor/insulator/conductor heterojunctions for photodetection. Nanotechnology, 2015, 26, 215203.	1.3	8
50	Sunlight absorbing titanium nitride nanoparticles. , 2015, , .		4
51	Tunable multiband metasurfaces by moiré nanosphere lithography. Nanoscale, 2015, 7, 20391-20396.	2.8	29
52	Selective patterned growth of ZnO nanowires/nanosheets and their photoluminescence properties. Optical Materials Express, 2015, 5, 353.	1.6	21
53	Active molecular plasmonics: tuning surface plasmon resonances by exploiting molecular dimensions. Nanophotonics, 2015, 4, 186-197.	2.9	26
54	Effect of different surfactants on structural and optical properties of Ce3+ and Tb3+ co-doped BiPO4 nanostructures. Optical Materials, 2015, 39, 110-117.	1.7	34

#	Article	IF	CITATIONS
55	Enhanced Multiphoton-Induced Luminescence in Silver Nanoparticles Fabricated with Nanosphere Lithography. Plasmonics, 2015, 10, 87-98.	1.8	4
56	Large Area, Aluminum Metal-Insulator-Metal Infrared Perfect Absorber. , 2014, , .		0
57	Large-area Tunable Al Plasmonic Substrate for Infrared Spectroscopy. , 2014, , .		0
58	Integrated plasmonic nanobiosensors. , 2013, , .		0
59	Dual-Band Perfect Absorber for Multispectral Plasmon-Enhanced Infrared Spectroscopy. ACS Nano, 2012, 6, 7998-8006.	7.3	459
60	Angle-and polarization-dependent collective excitation of plasmonic nanoarrays for surface enhanced infrared spectroscopy. Optics Express, 2011, 19, 11202.	1.7	27
61	Robust dithiocarbamate-anchored amine functionalization of Au nanoparticles. Journal of Nanoparticle Research, 2011, 13, 751-761.	0.8	24
62	Thin and Robust Encapsulation of Silver and Gold Nanoparticles with Dithiocarbamate-anchored Polyelectrolytes. Materials Research Society Symposia Proceedings, 2011, 1348, 140001.	0.1	0
63	Restricted meniscus convective self-assembly. Journal of Colloid and Interface Science, 2010, 344, 315-320.	5.0	55
64	Effect of the Interface in Plasmon-enhanced Second Harmonic Generation from Nonlinear Optical Thin Films. Materials Research Society Symposia Proceedings, 2010, 1248, 1120.	0.1	0
65	The Relationship between Growth Speed and Ambient Humidity in Convective Self-assembly. Materials Research Society Symposia Proceedings, 2010, 1273, 10701.	0.1	0
66	Interface effects in plasmon-enhanced second-harmonic generation from self-assembled multilayer films. Journal of the Optical Society of America B: Optical Physics, 2010, 27, 92.	0.9	7
67	Plasmon-Enhanced Second-Harmonic Generation from Ionic Self-Assembled Multilayer Films. Nano Letters, 2007, 7, 254-258.	4.5	81
68	Band-rejection and bandpass filters based on mechanically induced long-period fiber gratings. Microwave and Optical Technology Letters, 2004, 42, 15-17.	0.9	7
69	A novel interleaver based on dual-pass Mach-Zehnder interferometer. Microwave and Optical Technology Letters, 2004, 42, 253-255.	0.9	3
70	Mass Fabrication of WS <sub>2</sub> Nanodisks and their Scattering Properties. Advanced Materials Technologies, 0, , 2200432.	3.0	2